

Pseudogaps in Strongly Correlated Metals: Optical Conductivity within the Generalized Dynamical Mean-Field Theory Approach

E. Z. Kuchinskii, I. A. Nekrasov, M. V. Sadovskii

Institute for Electrophysics, Russian Academy of Sciences, Ekaterinburg, 620016, Russia

Abstract

Optical conductivity of the weakly doped two-dimensional repulsive Hubbard model on the square lattice with nearest and next nearest hoppings is calculated within the generalized dynamical mean field (DMFT+ χ_p) approach which includes correlation length scale into the standard DMFT equations via the momentum dependent self-energy χ_p , with full account of appropriate vertex corrections. This approach takes into consideration non-local dynamical correlations induced e.g. by short-ranged collective SDW (like antiferromagnetic spin fluctuations, which (at high enough temperatures) can be viewed as a quenched Gaussian random field with finite correlation length ξ). The DMFT effective single impurity problem is solved by numerical renormalization group (NRG). We consider both the case of correlated metal with the bandwidth $W \ll U$ and that of doped Mott insulator with $U \ll W$ (U — value of local Hubbard interaction). Optical conductivity calculated within DMFT+ χ_p demonstrates typical pseudogap behavior within the quasiparticle band in qualitative agreement with experiments in copper oxide superconductors. For large values of U pseudogap anomalies are effectively suppressed.

PACS numbers: 71.10.Fd, 71.10.Hf, 71.27.+a, 71.30.+h, 74.72.-h

I. INTRODUCTION

Pseudogap state is a major anomaly of electronic properties of underdoped copper oxides^{1,2}. We believe that the preferable "scenario" for its formation is most likely based on the model of strong scattering of electrons by short-ranged antiferromagnetic (AFM, SDW) spin fluctuations². This scattering mainly transfers momenta of the order of $Q = (\frac{\pi}{a}; \frac{\pi}{a})$ (a \parallel lattice constant of two dimensional lattice) leading to the formation of structures in the one-particle spectrum, which are precursors of the changes in the spectra due to long-range AFM order (period doubling) with non-Fermi liquid like behavior of spectral density in the vicinity of the so called "hot-spots" on the Fermi surface, appearing at intersections of the Fermi surface with antiferromagnetic Brillouin zone boundary (umklapp surface)².

In recent years a simplified model of the pseudogap state was studied^{3,4} under the assumption that the scattering by dynamic spin fluctuations can be reduced for high enough temperatures to a static Gaussian random field (quenched disorder) of pseudogap fluctuations. These fluctuations are defined by a characteristic scattering vectors of the order of Q , with distribution width determined by the inverse correlation length of short-range order $\propto 1/\xi$, and by appropriate energy scale (typically of the order of crossover temperature T^* to the pseudogap state²).

It is also well known that undoped cuprates are antiferromagnetic Mott insulators with $U \gg W$ ($U \parallel$ value of local Hubbard interaction, $W \parallel$ bandwidth of non-interacting band), so that correlation effects are very important and underdoped (and probably also optimally doped) cuprates are actually typical strongly correlated metals.

The cornerstone of the modern theory of strongly correlated systems is the dynamical mean-field theory (DMFT)^{5,6,7,8,9}. At the same time, standard DMFT is not appropriate for the "antiferromagnetic" scenario of pseudogap formation in strongly correlated metals due to the basic approximation of the DMFT, which completely neglects non-local dynamical correlation effects.

Different extensions of DMFT were proposed in recent years to cure this deficiency, such as extended DMFT (EDMFT)^{10,11}, which locally includes coupling to non-local dynamical fluctuations, and, most importantly, different versions the so-called cluster mean-field theories, such as the dynamical cluster approximation (DCA)¹² and cellular DMFT (CDMFT)¹³. However, these approaches have certain drawbacks. First of all, the effective quantum single

impurity problem becomes rather complex. Thus, majority of computational tools available for the DMFT can be used only for small enough clusters¹², i.e. include mostly nearest-neighbor fluctuations. It is especially difficult to apply these methods to calculations of two-particle properties, e.g. optical conductivity.

Recently we have proposed generalized DMFT+ p approach^{14,15,16}, which on the one hand retains the single-impurity description of the DMFT, with a proper account for local correlations and the possibility to use impurity solvers like NRG^{25,26}, while on the other hand, includes non-local correlations on a non-perturbative model basis, which allows to control characteristic scales and also types of non-local fluctuations. This latter point allows for a systematic study of the influence of non-local fluctuations on the electronic properties and in particular provides valuable hints on physical origin and possible interpretation of results. Within this approach we have studied single-particle properties, such as pseudogap formation in the density of states of the quasiparticle band both for correlated metal and doped Mott insulator, evolution of non-Fermi liquid like spectral density and ARPES spectra¹⁵, "destruction" of Fermi surfaces and formation of Fermi arcs¹⁴, as well as impurity scattering effects¹⁶. This formalism was also combined with modern LDA+DMFT calculations of electronic structure of "realistic" correlated systems to formulate LDA+DMFT+ p approach, which was applied for the description of pseudogap behavior in $\text{Bi}_2\text{Ca}_2\text{SrCu}_2\text{O}_8$ ¹⁷.

In this paper we develop our DMFT+ p approach for calculations of two-particle properties, such as (dynamic) optical conductivity, which is conveniently calculated within the standard DMFT^{7,8}. We show that inclusion of non-local correlations (pseudogap fluctuations) with characteristic length scale allows the description of pseudogap effects in longitudinal conductivity of the two-dimensional Hubbard plane.

The paper is organized as follows: In section II we present a short description of our DMFT+ p approach. In section III we derive basic DMFT+ p expressions for dynamic (optical) conductivity, as well as formulate recurrence equations to calculate the p -dependent self-energy and appropriate vertex part, which take into account all the relevant Feynman diagrams of perturbation series over pseudogap fluctuations. Computational details and basic results for optical conductivity are given in section IV. We also compare our results with that of the standard DMFT. The paper is ended with a summary section V including a short overview of related experimental results.

II. BASICS OF DMFT+_p APPROACH

As noted above the basic shortcoming of the traditional DMFT approach^{5,6,7,8,9} is the neglect of momentum dependence of electron self-energy. To include non-local effects, while remaining within the usual "single impurity analogy", we have proposed^{14,15,16} the following (DMFT+_p) approach. First of all, Matsubara "time" Fourier transformed single-particle Green function of the Hubbard model in obvious notations is written as:

$$G(i''; p) = \frac{1}{i'' + \Sigma(i'') + \Sigma_p(i'')}; \quad \Sigma = T(2n + 1); \quad (1)$$

where $\Sigma(i'')$ is the local contribution to self-energy, of DMFT type (surviving in the limit of spatial dimensionality $d \rightarrow 1$), while $\Sigma_p(i'')$ is some momentum dependent part. This last contribution can be due either to electron interactions with some "additional" collective modes or order parameter fluctuations, or may be induced by similar non-local contributions within the Hubbard model itself. No doublecounting problem arises in this approach, as discussed in details in Ref.¹⁵. At the same time our procedure as stressed in Refs.^{14,15,16} does not represent any systematic $1/d$ expansion. Basic assumption here is the neglect of all interference processes of the local Hubbard interaction and non-local contributions owing to these additional scatterings (non-crossing approximation for appropriate diagrams)¹⁵, as illustrated by diagrams in Fig. 1.

The self-consistency equations of generalized DMFT+_p approach are formulated as follows^{14,15}:

1. Start with some initial guess of local self-energy $\Sigma(i'')$, e.g. $\Sigma(i'') = 0$.
2. Construct $\Sigma_p(i'')$ within some (approximate) scheme, taking into account interactions with collective modes or order parameter fluctuations which in general can depend on (i') and β .

3. Calculate the local Green function

$$G_{ii}(i'') = \frac{1}{N} \sum_p \frac{1}{i'' + \Sigma(i'') + \Sigma_p(i'')}; \quad (2)$$

4. Define the "Weiss field"

$$G_0^{-1}(i'') = i'' + \Sigma(i'') + G_{ii}^{-1}(i''); \quad (3)$$

5. Using some "impurity solver" calculate the single-particle Green function $G_d(i'')$ for the effective Anderson impurity problem, placed at lattice site i , and defined by effective action which is written, in obvious notations, as:

$$S_e = \sum_0^Z d_{i1} \sum_0^Z d_{i2} c_{i1} G_0^{-1}(i_1 - i_2) c_{i1}^\dagger(i_2) + \sum_0^Z d_{iU} n_{i\uparrow}(i) n_{i\downarrow}(i): \quad (4)$$

6. Define a new local self-energy

$$\Sigma(i!) = G_0^{-1}(i!) - G_d^{-1}(i!): \quad (5)$$

7. Using this self-energy as "initial" one in step 1, continue the procedure until (and if) convergency is reached to obtain

$$G_{ii}(i'') = G_d(i''): \quad (6)$$

Eventually, we get the desired Green function in the form of (1), where $\Sigma(i'')$ and $\chi_p(i'')$ are those appearing at the end of our iteration procedure.

III. OPTICAL CONDUCTIVITY IN DMFT+ χ_p

A. Basic expressions for optical conductivity

To calculate dynamic conductivity we use the general expression relating it to retarded density-density correlation function $\chi^R(i!; q)^{18,19}$:

$$\sigma(i!) = \lim_{q! \rightarrow 0} \frac{ie^2 i!}{q^2} \chi^R(i!; q); \quad (7)$$

where e is electronic charge.

Consider full polarization loop graph in Matsubara representation shown in Fig. 2(a), which is conveniently (with explicit frequency summation) written as:

$$\chi(i!; q) = \sum_{n=0}^X \chi_{i''i''0}(i!; q) \sum_{n''=0}^X \chi_{i''}(i!; q) \quad (8)$$

and contains all possible interactions of our model, described by the full vertex part of Fig. 2(b). Note that, we use slightly unusual definition of the vertex part to include the

loop contribution without vertex corrections, which shortens further diagrammatic expressions. Retarded density-density correlation function is determined by appropriate analytic continuation of this loop and can be written as:

$$\chi^R(i!; q) = \frac{1}{2} \int_{-1}^1 d\omega [f(\omega_+) - f(\omega_-)] \chi^{RA}(q; i!) + f(\omega_+) \chi^{RR}(q; i!) - f(\omega_-) \chi^{AA}(q; i!); \quad (9)$$

where $f(\omega)$ { Fermi distribution, $\omega = \omega - \frac{i}{2}$, while two-particle loops $\chi^{RA}(q; i!)$, $\chi^{RR}(q; i!)$, $\chi^{AA}(q; i!)$ are determined by appropriate analytic continuations ($i\omega \rightarrow \omega + i0$ or $\omega - i0$) in (8). Then we can conveniently write dynamic conductivity as:

$$\sigma(i!) = \lim_{q \rightarrow 0} \frac{e^2}{2} \int_{-1}^1 d\omega [f(\omega_+) - f(\omega_-)] \chi^{RA}(q; i!) - \chi^{RA}(0; i!) + f(\omega_+) \chi^{RR}(q; i!) - \chi^{RR}(0; i!) - f(\omega_-) \chi^{AA}(q; i!) + \chi^{AA}(0; i!); \quad (10)$$

where the total contribution of additional terms with zero q can be shown (with the use of general Ward identities²⁰) to be zero.

To calculate $\chi_{i!i!0}^R(i!; q)$, entering the sum over Matsubara frequencies in (8), in DMFT+ γ_p approximation, which neglects interference between local Hubbard interaction and non-local contributions due to additional scatterings, e.g. by SDW pseudogap fluctuations¹⁵, we can write down Bethe-Salpeter equation, shown diagrammatically in Fig. 3, where we have introduced irreducible (local) vertex $U_{i!i!0}(i!)$ of DMFT and "rectangular" vertex, defined as in Fig. 2 (b) and containing all interactions with fluctuations. Analytically this equation can be written as:

$$\chi_{i!i!0}^R(i!; q) = \chi_{i!i!0}^R(i!; q)_{\text{non}} + \chi_{i!i!0}^R(i!; q) \sum_{i!0} U_{i!i!0}(i!) \chi_{i!0i!0}^R(i!; q); \quad (11)$$

where $\chi_{i!i!0}^R(i!; q)$ is the desired function calculated neglecting vertex corrections due to Hubbard interaction (but taking into account all non-local interactions with fluctuations, considered here to be static). Note that all q -dependence here is determined by $\chi_{i!i!0}^R(i!; q)$ as the vertex $U_{i!i!0}(i!)$ is local and q -independent.

As is clear from (10), to calculate conductivity, we need only to find \hat{q} -contribution to $\chi(i!; q)$ defined in (8). This can be done in the following way. First of all, note that all the loops in (11) contain q -dependence starting from terms of the order of q^2 . Then we can take an arbitrary loop (cross-section) in the expansion of (11) (see Fig. 3), calculating it up to terms of the order of q^2 , and make resummation of all contributions to the right and to the

left from this cross-section (using the obvious left { right symmetry of diagram summation in Bethe { Salpeter equation), putting $q = 0$ in all these graphs. This is equivalent to simple q^2 -differentiation of the expanded version of Eq. (11). This procedure immediately leads to the following relation for q^2 -contribution to (8):

$$(i!) \lim_{q \rightarrow 0} \frac{(i!; q)}{q^2} = \sum_{i''} \frac{(i!; 0)}{q^2} = \sum_{i''} \frac{0_{i''}(i!; q=0)}{q^2} \quad (12)$$

where

$$0_{i''}(i!) = \lim_{q \rightarrow 0} \frac{0_{i''}(i!; q)}{q^2} \quad (13)$$

with $0_{i''}(i!; q)$ containing vertex corrections only due to non-local (pseudogap) fluctuations, while one-particle Green's functions in it are taken with self-energies due to both these fluctuations and local DMFT-like interaction, like in Eq. (1). The vertex $0_{i''}(i!; q=0)$ is determined diagrammatically as shown in Fig. 4, or analytically:

$$0_{i''}(i!; q=0) = 1 + \sum_{i'''} U_{i''i'''} 0_{i'''}(i!; q=0): \quad (14)$$

Now using Bethe-Salpeter equation (11) we can write explicitly:

$$\begin{aligned} 0_{i''}(i!; q=0) &= 1 + \sum_{i'''} \frac{0_{i'''}(i!; q=0)}{0_{i''}(i!; q=0)} = \\ &= \frac{\sum_{i'''} 0_{i'''}(i!; q=0)}{0_{i''}(i!; q=0)}: \end{aligned} \quad (15)$$

For $q = 0$ we have the following Ward identity, which can be obtained by direct generalization of the proof given in Refs.^{18,20} (see Appendix A):

$$(i!) 0_{i''}(i!; q=0) = (i!) \sum_{i'''} 0_{i'''}(i!; q=0) = \sum_p G(i'' + i!; p) \sum_p G(i''; p): \quad (16)$$

Denominator of (15) contains vertex corrections only from non-local correlations (e.g. pseudogap fluctuations), while Green's functions here are "dressed" both by these correlations and local (DMFT) Hubbard interaction. Thus we may consider the loop entering the denominator as dressed by (pseudogap) fluctuations only, but with "bare" Green's functions:

$$G_0(i''; p) = \frac{1}{i'' + \Pi(p)(i'')}; \quad (17)$$

where $\Pi(p)$ is local contribution to self-energy from DMFT. For this problem we have the following Ward identity, similar to (16) (see Appendix A):

$$\begin{aligned} \sum_p G(i'' + i!; p) \sum_p G(i''; p) &= 0_{i''}(i!; q=0) [(i'' + i!) - (i'') - i!] \\ &= 0_{i''}(i!; q=0) [(i!) - i!]; \end{aligned} \quad (18)$$

where we have introduced

$$(i!) = (i'' + i!) (i'') : \quad (19)$$

Thus, using (16), (18) in (15) we get the final expression for $i''(i!; q = 0)$:

$$i''(i!; q = 0) = 1 - \frac{(i!)}{i!} : \quad (20)$$

Then (12) reduces to:

$$(i!) = \sum_{i''}^X i''(i!) = 1 - \frac{(i!)}{i!} : \quad (21)$$

Analytic continuation to real frequencies is obvious and using (12), (21) in (10) we can write the final expression for the real part of dynamic conductivity as:

$$\text{Re}(\sigma(\omega)) = \frac{e^2}{2} \sum_{i=1}^Z d'' [f(\omega'') - f(\omega''_+)] \text{Re} \left(\frac{\sigma''^{\text{ORA}}(\omega)}{1 - \frac{\sigma''^{\text{R}}(\omega'_+) \sigma''^{\text{A}}(\omega'')^2}{i!}} \right) + \frac{\sigma''^{\text{ORR}}(\omega)}{1 - \frac{\sigma''^{\text{R}}(\omega'_+) \sigma''^{\text{R}}(\omega'')^2}{i!}} : \quad (22)$$

Thus we have achieved a great simplification of our problem. To calculate optical conductivity in DMFT+_p we only have to solve single-particle problem as described by DMFT+_p procedure above to determine self-consistent values of local self-energies σ'' , while non-trivial contribution of non-local correlations are to be included via (13), which is to be calculated in some approximation, taking into account only interaction with non-local (e.g. pseudogap) fluctuations, but using the "bare" Green's functions of the form (17), which include local self-energies already determined in the general DMFT+_p procedure. Actually (22) provides also an effective algorithm to calculate dynamic conductivity in standard DMFT (neglecting any non-local correlations), as (13) is then easily calculated from a simple loop diagram, determined by two Green's functions and free scalar vertices. As usual, there is no need to calculate vertex corrections within DMFT itself, as was proven first considering the loop with vector vertices^{7,8}.

B. Recurrence relations for self-energy and vertex parts.

As we are mainly interested in the pseudogap state of copper oxides, we shall further concentrate on the effects of scattering of electrons from collective short-range SDW (like antiferromagnetic spin) fluctuations. In a kind of a simplified approach, valid only for high

enough temperatures^{3,4} we shall calculate $\Sigma_p(i!)$ for an electron moving in the quenched random field of (static) Gaussian spin fluctuations with dominant scattering momentum transfers from the vicinity of some characteristic vector Q ("hot-spots" model²), using (as we have done in Refs.^{14,15,16}) slightly generalized version of the recurrence procedure proposed in^{3,4,21} (see also Ref.¹⁹), which takes into account all Feynman diagrams describing the scattering of electrons by this random field. In general, neglect of fluctuation dynamics, overestimates pseudogap effects. Referring the reader to earlier papers for details^{3,4,14,15,16}, here we just start with the main recurrence relation, determining the self-energy:

$$\Sigma_k(i!;p) = - \frac{s(k)}{i! + \Sigma_k(i!;p) + i v_k} : \quad (23)$$

Usually one takes the value of Σ_{k+1} for large enough k equal to zero and doing recurrence backwards to $k = 1$ gets the desired physical self-energy $\Sigma(i!;p) = \Sigma_1(i!;p)$ ^{4,19,21}.

In Eq. (23) $s(k)$ characterizes the energy scale and ξ^{-1} is the inverse correlation length of short-range SDW fluctuations, $\Sigma_k(p) = \Sigma(p + Q)$ and $v_k = j_{p+Q}^x j + j_{p+Q}^y j$ for odd k while $\Sigma_k(p) = \Sigma(p)$ and $v_k = j_p^x j + j_p^y j$ for even k . The velocity projections v_p^x and v_p^y are determined by usual momentum derivatives of the "bare" electronic energy dispersion $\Sigma(p)$. Finally, $s(k)$ represents a combinatorial factor, which here is always assumed to be that corresponding to the case of Heisenberg spin fluctuations in "nearly antiferromagnetic Fermi liquid" (spin-fermion (SF) model of Ref.³, SDW-type fluctuations):

$$s(k) = \begin{cases} 8 & \\ < \frac{k+2}{3} & \text{for odd } k \\ : \frac{k}{3} & \text{for even } k \end{cases} \quad (24)$$

As was stressed in Refs.^{15,16} this procedure introduces an important length scale not present in standard DMFT, which mimics the effect of short-range (SDW) correlations within fermionic "bath" surrounding the DMFT effective single Anderson impurity.

An important aspect of the theory is that both parameters ξ and ξ^{-1} can in principle be calculated from the microscopic model at hand¹⁵, but here we consider these as phenomenological parameters of the theory (e.g. to be determined from experiments).

Now to calculate optical conductivity we need the knowledge of the basic block $\Sigma_{i!}^0(i!;q)$, entering (13), or, more precisely, appropriate functions analytically continued to real frequencies: $\Sigma_{i!}^{ORA}(!;q)$ and $\Sigma_{i!}^{ORR}(!;q)$, which in turn define $\Sigma_{i!}^{ORA}(!)$ and $\Sigma_{i!}^{ORR}(!)$ entering (22),

and defined by obvious relations similar to (13):

$$\Gamma_{\text{A}}^{\text{OR A}}(\omega) = \lim_{q \rightarrow 0} \frac{\Gamma_{\text{A}}^{\text{OR A}}(\omega; q)}{q^2}; \quad (25)$$

$$\Gamma_{\text{R}}^{\text{OR R}}(\omega) = \lim_{q \rightarrow 0} \frac{\Gamma_{\text{R}}^{\text{OR R}}(\omega; q)}{q^2}; \quad (26)$$

By definition we have:

$$\begin{aligned} \Gamma_{\text{A}}^{\text{OR A}}(\omega; q) &= \sum_{\text{p}} G^{\text{R}}(\omega_+; p_+) G^{\text{A}}(\omega_-; p_-) \Gamma_{\text{A}}^{\text{RA}}(\omega; p_-; \omega_+; p_+) \\ \Gamma_{\text{R}}^{\text{OR R}}(\omega; q) &= \sum_{\text{p}} G^{\text{R}}(\omega_+; p_+) G^{\text{R}}(\omega_-; p_-) \Gamma_{\text{R}}^{\text{RR}}(\omega; p_-; \omega_+; p_+); \end{aligned} \quad (27)$$

which are shown diagrammatically in Fig. 5. Here Green's functions $G^{\text{R}}(\omega_+; p_+)$ and $G^{\text{A}}(\omega_-; p_-)$ are defined by analytic continuation ($i\omega \rightarrow \omega - i0$) of Matsubara Green's functions (1) determined by recurrence procedure (23), while vertices $\Gamma_{\text{A}}^{\text{RA}}(\omega; p_-; \omega_+; p_+)$ and $\Gamma_{\text{R}}^{\text{RR}}(\omega; p_-; \omega_+; p_+)$, containing all vertex corrections due to pseudogap fluctuations are given by the recurrence procedure, derived first (for one-dimensional case) in Ref.²² (see also Ref.¹⁹) and generalized for two-dimensional problem in Ref.²³ (see also Ref.³). The basic idea used here is that an arbitrary diagram for the vertex part can be obtained by an insertion of an "external field" line into the appropriate diagram for the self-energy^{22,23,24}. In our model we can limit ourselves only to diagrams with non-intersecting interaction lines with additional combinatorial factors $s(k)$ in "initial" interaction vertices^{3,4,21}. Thus, all diagrams for the vertex part are, in fact, generated by simple ladder diagrams with additional $s(k)$ factors, associated with interaction lines^{22,23} (see also¹⁹). Then we obtain the system of recurrence relations for the vertex part $\Gamma_{\text{A}}^{\text{RA}}(\omega; p_-; \omega_+; p_+)$ shown by diagrams of Fig. 6. Analytically it has the following form²³, where we now also included contributions due to local (DMFT) self-energies, originating from DMFT + p -loop:

$$\begin{aligned} \Gamma_{k-1}^{\text{RA}}(\omega; p_-; \omega_+; p_+) &= 1 + s(k) G_k^{\text{A}}(\omega_-; p_-) G_k^{\text{R}}(\omega_+; p_+) \\ &\quad \frac{1 + \frac{2i v_k k}{\omega_k(p_+) + \omega_k(p_-)} G_k^{\text{R}}(\omega_+) + G_k^{\text{A}}(\omega_-)}{\Gamma_k^{\text{RA}}(\omega; p_-; \omega_+; p_+)} \end{aligned} \quad (28)$$

and

$$G_k^{\text{RA}}(\omega; p_-) = \frac{1}{\omega_k(p_-) - i v_k k G_k^{\text{RA}}(\omega) - G_{k+1}^{\text{RA}}(\omega; p_-)}; \quad (29)$$

The "physical" vertex $\Gamma_{k=0}^{RA}(\omega; p; \omega_+; p_+)$ is determined as $\Gamma_{k=0}^{RA}(\omega; p; \omega_+; p_+)$. Recurrence procedure (28) takes into account all perturbation theory diagrams for the vertex part. For $\omega \neq 0$ ($\omega = 0$) (28) reduces to the series studied in Ref.²⁴ (cf. also Ref.³), which can be summed exactly in analytic form. Standard "ladder" approximation corresponds in our scheme to the case of combinatorial factors $s(k)$ in (28) being equal to 1^{22} .

Recurrence procedure for $\Gamma_{k=0}^{RR}(\omega; p_+; \omega_+; p_+)$ differs from (28) only by obvious replacements $A \rightarrow R$ and the whole expression in square brackets in the r.h.s. of (28) just replaced by 1:

$$\Gamma_{k=0}^{RR}(\omega; p; \omega_+; p_+) = 1 + \sum_k s(k) G_k^R(\omega; p) G_k^R(\omega_+; p_+) \Gamma_k^{RR}(\omega; p; \omega_+; p_+); \quad (30)$$

Note that DMFT (Hubbard) interaction enters these equations only via local self-energies $\Sigma_k^{RA}(\omega)$ calculated self-consistently according to our DMFT + Σ_p procedure.

Equations (1), (23), (28), (30) together with (25), (26) and (22) provide us with the complete self-consistent procedure to calculate optical conductivity of our model in DMFT + Σ_p approach.

IV. RESULTS AND DISCUSSION

A. Generalities

In the following, we shall discuss our results for a standard one-band Hubbard model on a square lattice. The "bare" electronic dispersion in tight-binding approximation, with the account of nearest (t) and next nearest (t') neighbour hoppings, is given by:

$$\epsilon(p) = -2t(\cos p_x a + \cos p_y a) - 4t' \cos p_x a \cos p_y a; \quad (31)$$

where a is the lattice constant. To be concrete, below we present results for $t = 0.25\text{eV}$ (more or less typical for cuprates) and $t' = -0.4$ (which gives Fermi surface similar to those observed in many cuprates).

For the square lattice the bare bandwidth is $W = 8t$. To study strongly correlated metallic state obtained as doped Mott insulator we have used the value for the Hubbard interaction $U = 40t$ and filling factors $n = 1.0$ (half-filling) and $n = 0.8$ (hole doping). For

correlated metal with W & U we have taken typical values like $U = 4t$, $U = 6t$ and $U = 10t$ for U & W . Calculations were performed for different fillings: half-filling ($n = 1.0$) and for $n = 0.8; 0.9$ (hole doping). As typical values for t we have chosen $t = t$ and $t = 2t$ and for correlation length $\xi = 2a$ and $\xi = 10a$ (motivated mainly by experimental data for cuprates^{2,3}).

To solve an effective Anderson impurity problem of DMFT we applied a reliable numerically exact method of numerical renormalization group (NRG)^{25,26}, which, actually, allowed us to work with real frequencies from the very beginning, overcoming possible difficulties of performing analytical continuation numerically. Calculations were performed for two different temperatures: $T = 0.088t$ and $T = 0.356t$.

All necessary integrations were done directly, e.g. over the whole Brillouin zone (with the account of obvious symmetries), or wide enough frequency range. Integration moments are made dimensionless in a natural way with the help of the lattice constant a . Conductivity is measured in units of the universal conductivity in two dimensions: $\sigma_0 = \frac{e^2}{\hbar} = 2.5 \cdot 10^{-4} \text{ Ohm}^{-1}$.

B. Optical conductivity in standard DMFT

Optical conductivity was calculated for different combinations of parameters of the model. Below we present only a fraction of our results, which are, probably, most relevant for copper oxides. We shall start with presenting some typical results, obtained within our formalism in conventional DMFT approximation, neglecting pseudogap fluctuations, just to introduce the basic physical picture and demonstrate the effectiveness of our approach.

Characteristic feature of the strongly correlated metallic state is the coexistence of lower and upper Hubbard bands splitted by the value of U with a quasiparticle peak at the Fermi level^{7,8}. For the case of strongly correlated metal with W & U we observe almost no contribution from excitations to upper Hubbard model in optical conductivity, as can be seen in Fig. 7 (where we show the real part of conductivity $\text{Re}(\sigma(\omega))$). This contribution is almost completely masked by a typical Drude-like frequency behavior, with only slightly non-monotonous behavior for $\omega < U$, which completely disappears as we rise the temperature.

Situation is different in doped Mott insulator with $U > W$. In Fig. 8 we clearly observe an additional maximum of optical absorption for $\omega < U$, however, at smaller frequencies we

again observe typical Druide-like behavior, slightly non-monotonous for small frequencies due to quasiparticle band formation (see insert in Fig. 8).

These and similar results are more or less well known from the previous studies^{7,8}, and are quoted here only to demonstrate the consistency of our formalism and to prepare the reader for new results, showing pseudogap behavior.

C. Optical conductivity in DMFT + p

1. Correlated metal

Let us start the discussion of results obtained within our generalized DMFT + p approach for the case of W & U .

In Fig. 9 we show our DMFT + p results for the real part of optical conductivity for correlated metal ($U = 4t$) for two values of temperature, compared with similar data without pseudogap fluctuations (pure DMFT). We clearly observe formation of typical pseudogap (absorption) anomaly on the "shoulder" of Druide-like peak, which is partially "filled" with the growth of temperature. This behavior is quite similar to "mid-infrared feature" that is observed in optical conductivity of cuprate superconductors^{27,28}. In Fig. 10 we show the behavior of $\text{Re}(\sigma)$ for different values of the pseudogap amplitude Δ . We see that pseudogap anomaly naturally grows with the growth of Δ . Fig. 11 illustrates the dependence of $\text{Re}(\sigma)$ on correlations length of pseudogap (AFM, SDW) fluctuations. Again we observe the natural behavior | pseudogap anomaly is "filled" for shorter correlation lengths, i.e. as fluctuations become more short-ranged. At last, in Fig. 12 we demonstrate dependence of pseudogap anomaly in optical conductivity on correlation strength, i.e. on Hubbard interaction U . It is seen that the frequency range, where pseudogap anomaly is observed becomes narrower as correlation strength grows. This correlates with general narrowing of the pseudogap anomaly and spectral densities with the growth of correlations, observed in our previous work^{15,16}. For large values of U pseudogap anomaly is practically suppressed. This is the main qualitative difference of the results of the present approach, compared to our earlier work²³ on optical conductivity in the pseudogap state. Comparing the data of present work for $U = 0$ with similar data of Ref.²³, it should be noted, that in this earlier work we have performed calculations of dynamic conductivity only for $T = 0$ and used

simplified expressions, neglecting $RR;AA$ loops contributions to conductivity, as well as small frequency expansion¹⁸, just to speed up calculations. These simplifications lead to some quantitative differences with the results of present work, where all calculations are done exactly using the general expression (22), though qualitatively the frequency behavior of conductivity is the same.

2. Doped Mott insulator

Now we shall discuss our results for the case of doped Mott insulator with $U = W$. This case has no direct relevance to copper oxides, but is interesting from the general point of view and we present some of our results.

The real part of optical conductivity for the case of $U = 40t$ is shown in Figs. 13,14.

In Fig. 13 we show $\text{Re}(\sigma)$ for doped Mott insulator in DMFT+ ϕ approach several values of pseudogap amplitude Δ . Obviously enough, pseudogap fluctuations lead to significant changes of optical conductivity only for relatively small frequencies of the order of t , while for high frequencies (e.g. of the order of U , where the upper Hubbard band contributes) we do not observe pseudogap effects (see insert in Fig. 13). For small frequencies we observe pseudogap suppression of Drude-like peak, with only a shallow anomaly for $\Delta = 0$, which just disappears for smaller values of Δ or shorter correlation lengths.

In Fig. 14 we show the similar data for the special case of $t^0 = 0$ and $n = 1$, i.e. at half-filling (Mott insulator) for different values of inverse correlation length $\kappa = 1/\xi$. Conductivity at small frequencies is determined only by thermal excitations and pseudogap fluctuations suppress it significantly. Shorter correlation lengths obviously lead to larger values of conductivity at small frequencies. Transitions to upper Hubbard band are not affected by these fluctuations at all.

V. CONCLUSION

The present work is the direct continuation of our previous work^{14,15,16}, where we have proposed a generalized DMFT+ ϕ approach, which is meant to take into account the important effects of non-local correlations (in principle of any type) in addition to the (essentially exact) treatment of local dynamical correlations by DMFT. Here we used a generalized

DMFT+ μ approach to calculate dynamic (optical) conductivity of two-dimensional Hubbard model with pseudogap fluctuations. Our results demonstrate, that pseudogap anomalies observed in optical conductivity of copper oxides can, in principle, be explained by this model. Main advantage in comparison to the previous work²³ is our ability now to study the role of strong electronic correlations, which are decisive in the formation of electronic structure of systems like copper oxides. In fact, we have demonstrated an important suppression of pseudogap anomaly in optical conductivity with the growth of correlation strength.

As we already noted in Ref.¹⁵ qualitatively similar results on pseudogap formation in single-particle characteristics for the 2d Hubbard model were also obtained within cluster extensions of DMFT^{12,13}. However, these methods have generic restrictions concerning the size of the cluster, and up to now were not widely applied to calculations of two-particle properties, such as general response functions, and, in particular, to calculations of dynamic (optical) conductivity.

Our approach is free of these limitations, though for the price of introduction of additional (semi) phenomenological parameters (correlation length ξ , and pseudogap amplitude Δ). It is much less time consuming, thus its advantage for calculations of two-particle response functions is obvious. It also opens the possibility of systematic comparison of different types of non-local fluctuations and their effects on electronic properties, providing more intuitive way to analyze experiments or theoretical data obtained within more advanced schemes. Note, again, that in principle both ξ and Δ can be calculated from the original model¹⁵. Our scheme works for any Coulomb interaction strength U , pseudogap strength Δ , correlation length ξ , filling n and bare electron dispersion $\epsilon(k)$.

The present formalism can be easily generalized in the framework of our recently proposed LDA+DMFT+ μ approach, which will allow to perform calculations of pseudogap anomalies of optical conductivity for realistic models. It can also be easily generalized to orbital degrees of freedom, phonons, impurities, etc.

VI. ACKNOWLEDGEMENTS

We are grateful to Th. Pruschke for providing us with his effective NRG code. This work was supported in part by RFBR grants 05-02-16301 (MSEK,IN), 05-02-17244 (IN), 06-02-90537 (IN), by the joint UR0-SO project (EK,IN), and programs of the Presidium

of the Russian Academy of Sciences (RAS) "Quantum macrophysics" and of the Division of Physical Sciences of the RAS "Strongly correlated electrons in semiconductors, metals, superconductors and magnetic materials". I.N. acknowledges support from the Dynasty Foundation and International Center for Fundamental Physics in Moscow program for young scientists and also from the grant of President of Russian Federation for young PhD MK-2118.2005.02.

APPENDIX A: WARD IDENTITIES

In this Appendix we present derivation of Ward identities used in the main text. Let us start with the general expression for variation of electron self-energy due to an arbitrary variation of the complete Green's function, which is valid for any interacting Fermi system²⁹:

$$\Gamma_p = \sum_{p^0} U_{pp^0}(q) G_{p^0}; \quad (A1)$$

where $U_{pp^0}(q)$ is an irreducible vertex in particle-hole channel, and we use 4-dimensional notations $p = (i''; p)$, $q = (i'; q)$ etc. In the following we take:

$$p = p_+ + p_- \quad (i''; p_+) \quad (i''; p_-) \quad (A2)$$

and (in the same notations):

$$G_p = G_+ + G_- = (G_+ G_-)_p (G_0^{-1})_p; \quad (A3)$$

where $(G_0^{-1})_p = G_{0+}^{-1} - G_{0-}^{-1}$, and the last expression was obtained using the standard Dyson equation.

Note the similarity of Eq. (A1) to the Ward identity for non-interacting electrons in the impure system, derived in Ref.¹⁸.

Now substituting the last expression in (A3) we get:

$$\Gamma_p = \sum_{p^0} U_{pp^0}(q) (G_+ G_-)_{p^0} (G_0^{-1})_{p^0}; \quad (A4)$$

Iterating this equation we obtain:

$$\begin{aligned} \Gamma_p = & \sum_{p^0} U_{pp^0}(G_+ G_-)_{p^0} (G_0^{-1})_{p^0} + \\ & + \sum_{p^{00}} U_{pp^{00}}(G_+ G_-)_{p^{00}} U_{p^{00}p^0}(G_+ G_-)_{p^0} (G_0^{-1})_{p^0} + \dots : \end{aligned} \quad (A5)$$

Multiplying both sides of (A 5) by $(G + G_p)_{p^0}$ and adding

$$\sum_{p^0} (G + G_p)_{p^0} (G_0^{-1})_{p^0} = (G + G_p) (G_0^{-1})_p$$

we have:

$$\begin{aligned} (G + G_p) (G_0^{-1})_p &= \sum_{p^0} [(G + G_p)_{p^0} + (G + G_p) U_{pp^0} (G + G_p)_{p^0} + \\ &+ (G + G_p) \sum_{p^{00}} U_{pp^{00}} (G + G_p)_{p^{00}} U_{p^{00}p^0} (G + G_p)_{p^0} + \dots] (G_0^{-1})_{p^0} = \\ &= \sum_{p^0} \gamma_{pp^0}(q) (G_0^{-1})_{p^0}; \end{aligned} \quad (A 6)$$

where $\gamma_{pp^0}(q)$ is the complete two { particle Green's function determined by the following Bethe { Salpeter equation²⁹:

$$\gamma_{pp^0}(q) = (G + G_p)_{p^0} + (G + G_p) \sum_{p^0} U_{pp^0} \gamma_{pp^0}(q); \quad (A 7)$$

Finally we obtain:

$$G_p = \sum_{p^0} \gamma_{pp^0}(q) (G_0^{-1})_{p^0}; \quad (A 8)$$

which is the general form of our Ward identity.

Summing both sides of (A 8) over p and taking $q = 0$ we obtain the identity (16) used above. Similarly, taking the "bare" Green's function (17) we obtain (18).

-
- ¹ T. Timusk, B. Statt, *Rep. Progr. Phys.*, 62, 61 (1999).
- ² M. V. Sadovskii, *Usp. Fiz. Nauk* 171, 539 (2001) [*Physics (Uspekhi)* 44, 515 (2001)].
- ³ J. Schmalian, D. Pines, B. Stojkovic, *Phys. Rev. Lett.* 80, 3839 (1998); *Phys. Rev. B* 60, 667 (1999).
- ⁴ E. Z. Kuchinskii, M. V. Sadovskii, *Zh. Eksp. Teor. Fiz.* 115, 1765 (1999) [*JETP* 88, 347 (1999)].
- ⁵ W. Metzner and D. Vollhardt, *Phys. Rev. Lett.* 62, 324 (1989).
- ⁶ D. Vollhardt, in *Correlated Electron Systems*, edited by V. J. Emery, World Scientific, Singapore, 1993, p. 57.
- ⁷ Th. Pruschke, M. Jarrell, and J. K. Freericks, *Adv. in Phys.* 44, 187 (1995).
- ⁸ A. Georges, G. Kotliar, W. Krauth, and M. J. Rozenberg, *Rev. Mod. Phys.* 68, 13 (1996).
- ⁹ G. Kotliar and D. Vollhardt, *Physics Today* 57, No. 3 (March), 53 (2004).
- ¹⁰ Q. Si and J. L. Smith, *Phys. Rev. Lett.* 77, 3391 (1996).
- ¹¹ EDMFT approach to pseudogap formation can be found in K. Haule, A. Rosch, J. Kroha, and P. Wölfe, *Phys. Rev. Lett.* 89, 236402 (2002); K. Haule, A. Rosch, J. Kroha, and P. Wölfe, *Phys. Rev. B* 68, 155119 (2003).
- ¹² Th. Maier, M. Jarrell, Th. Pruschke and M. Hettler, *Rev. Mod. Phys.* 77, 1027 (2005).
- ¹³ G. Kotliar, S. Y. Savrasov, G. Palsson, G. Biroli, *Phys. Rev. Lett.* 87, 186401 (2001); M. Capone, M. Civelli, S. S. Kancharla, C. Castellani, and G. Kotliar, *Phys. Rev. B* 69, 195105 (2004).
- ¹⁴ E. Z. Kuchinskii, I. A. Nekrasov, M. V. Sadovskii, *Pis'ma Zh. Eksp. Teor. Fiz.* 82, 217 (2005) [*JETP Lett.* 82, 198 (2005)].
- ¹⁵ M. V. Sadovskii, I. A. Nekrasov, E. Z. Kuchinskii, Th. Pruschke, V. I. Anisimov, *Phys. Rev. B* 72, 155105 (2005).
- ¹⁶ E. Z. Kuchinskii, I. A. Nekrasov, M. V. Sadovskii, *Fizika Nizkikh Temperatur* 32, 528 (2006) [*Low Temp. Phys.* 32, 398 (2006)].
- ¹⁷ E. Z. Kuchinskii, I. A. Nekrasov, Z. V. Pchelkina, M. V. Sadovskii, *arXiv: cond-mat/0606651*.
- ¹⁸ D. Vollhardt, *P. Wölfe. Phys. Rev. B* 22, 4666 (1980).
- ¹⁹ M. V. Sadovskii, *Diagrammatics*. World Scientific, Singapore 2006.
- ²⁰ V. Janis, J. Kobrenc, V. Spicka, *Eur. J. Phys. B* 35, 77 (2003).

- ²¹ M . V . Sadovskii, Zh. Eksp. Teor. Fiz. 77, 2070 (1979) [Sov Phys. {JETP 50, 989 (1979)}].
- ²² M . V . Sadovskii, A . A . Timofeev. J. Moscow Phys. Soc. 1, 391 (1991).
- ²³ M . V . Sadovskii, N . A . Strigina. Zh. Eksp. Teor. Phys. 122, 610 (2002) [JETP 95, 526 (2002)].
- ²⁴ M . V . Sadovskii. Zh. Eksp. Teor. Fiz. 66, 1720 (1974)) [Sov. Phys. { JETP 39, 845 (1974)}].
- ²⁵ K . G . Wilson, Rev. Mod. Phys. 47, 773 (1975); H . R . Krishna-murthy, J . W . Wilkins, and K . G . Wilson, Phys. Rev. B 21, 1003 (1980); *ibid.* 21, 1044 (1980); A . C . Hewson, The Kondo Problem to Heavy Fermions (Cambridge University Press, 1993).
- ²⁶ R . Bulla, A . C . Hewson and Th. Pruschke, J. Phys. { Condens. Matter 10, 8365 (1998); R . Bulla, Phys. Rev. Lett. 83, 136 (1999).
- ²⁷ D . N . Basov, T . T . Imusk. Rev. Mod. Phys. 77, 721 (2005).
- ²⁸ J . Hwang, T . T . Imusk, G . D . Gu. ArXiv: cond-mat/0607653.
- ²⁹ A . B . Migdal. Theory of Finite Fermi Systems and Applications to Atomic Nuclei. Interscience Publishers. NY 1967.

FIGURES

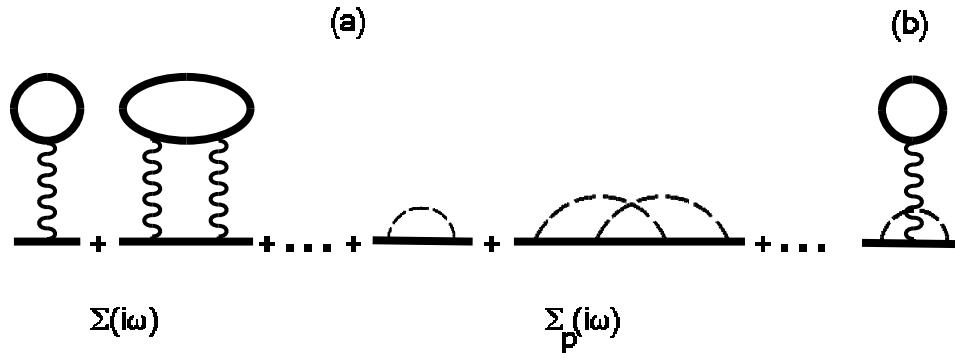


FIG. 1: Typical "skeleton" diagrams for the self-energy in the DMFT + p approach. The first two terms are examples of DMFT self-energy diagrams; the middle two diagrams show some contributions to the non-local part of the self-energy (e.g. from spin fluctuations) represented as dashed lines; the last diagram (b) is an example of neglected diagrams leading to interference between the local and non-local parts.

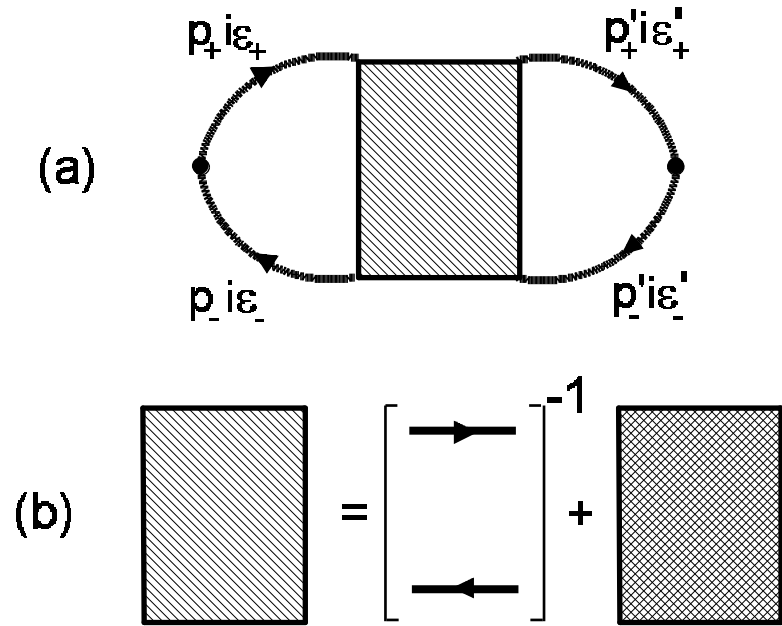


FIG. 2: Full polarization loop (a) with vertex part, which includes free electron contribution in addition to the standard vertex, containing all interactions (b). Here $p_+ = p - \frac{g}{2}$, $p_- = p + \frac{g}{2}$.

$$\begin{aligned}
& \text{Shaded Loop} = \text{Unshaded Loop} + \\
& + \text{Unshaded Loop} \circledast \text{U} \circledast \text{Unshaded Loop} + \\
& + \text{Unshaded Loop} \circledast \text{U} \circledast \text{Unshaded Loop} \circledast \text{U} \circledast \text{Unshaded Loop} + \dots = \\
& = \text{Unshaded Loop} + \text{Unshaded Loop} \circledast \text{U} \circledast \text{Shaded Loop}
\end{aligned}$$

FIG. 3: Bethe-Salpeter equation for polarization loop in DMFT + p approach. Circle represents irreducible vertex part of DMFT, which contains only local interactions, surviving in the limit of $d \rightarrow 1$. Unshaded rectangular vertex represents non-local interactions, e.g. with SDW (pseudo-gap) fluctuations, which is defined similarly to Fig. 2(b).

$$\begin{aligned}
\gamma_{i\varepsilon}(i\omega, \mathbf{q}=0) &= 1 + \text{[Diagram 1]} + \\
&+ \text{[Diagram 2]} + \dots = \\
&= 1 + \text{[Diagram 3]}
\end{aligned}$$

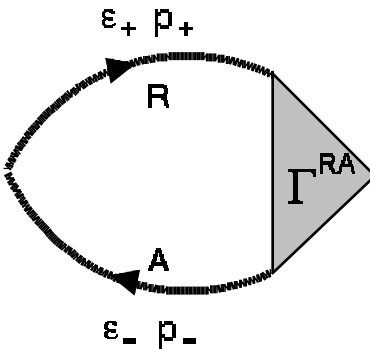
The diagrams are as follows:

 Diagram 1: A horizontal rectangle with two vertical lines inside. The left half has a curved arrow pointing right, and the right half has a curved arrow pointing left. To the right of the rectangle is a circle labeled 'U' with two external lines.

 Diagram 2: A horizontal rectangle with two vertical lines inside. The left half has a curved arrow pointing right, and the right half has a curved arrow pointing left. To the right of the rectangle is a circle labeled 'U' with two external lines. To the right of this circle is another identical rectangle with curved arrows, followed by another circle labeled 'U' with two external lines.

 Diagram 3: A horizontal rectangle with two vertical lines inside. The left half has a curved arrow pointing right, and the right half has a curved arrow pointing left. The central vertical line is shaded with diagonal lines. To the right of the rectangle is a circle labeled 'U' with two external lines.

FIG. 4: Effective vertex $\gamma_{i\varepsilon}(i\omega; \mathbf{q} = 0)$ used in calculations of conductivity.

$$\Phi_{\varepsilon}^{0RA}(q, \omega) =$$


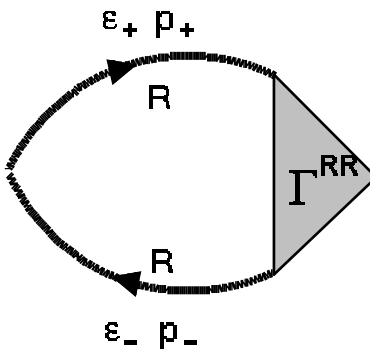
$$\Phi_{\varepsilon}^{0RR}(q, \omega) =$$


FIG. 5: Diagrammatic representation of $\Phi_{\varepsilon}^{0RA}(q, \omega)$.

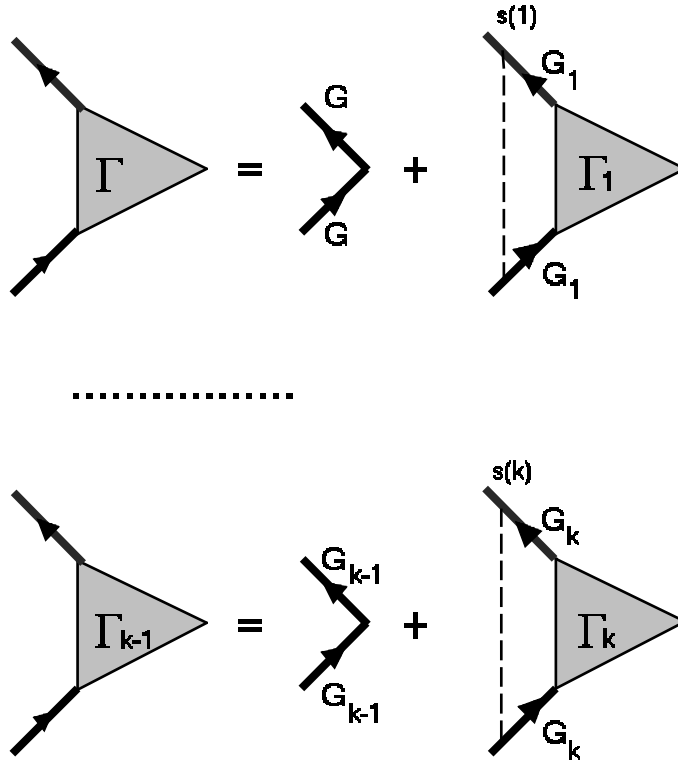


FIG . 6: Recurrence relations for the vertex part. Dashed lines denote s .

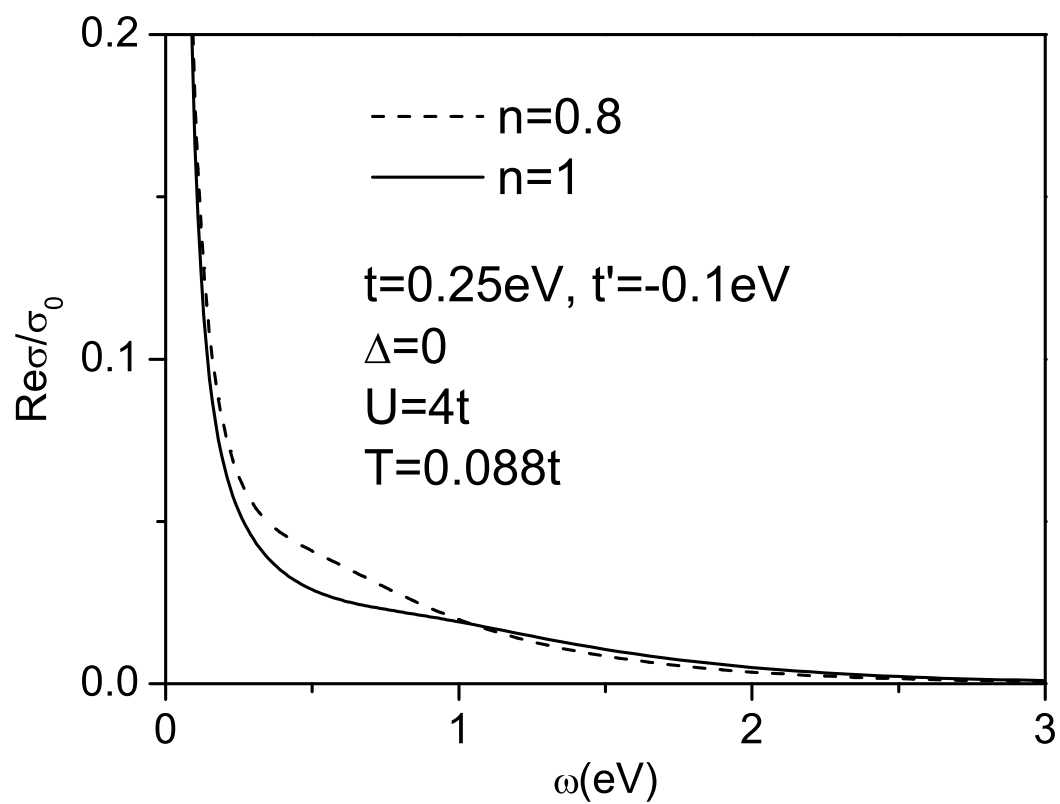


FIG. 7: Real part of optical conductivity for correlated metal ($U = 4t$, $t' = -0.4t$, $t = 0.25$ eV) in DMFT approximation for two values of filling factor: $n = 1$ and $n = 0.8$. Temperature $T = 0.088t$.

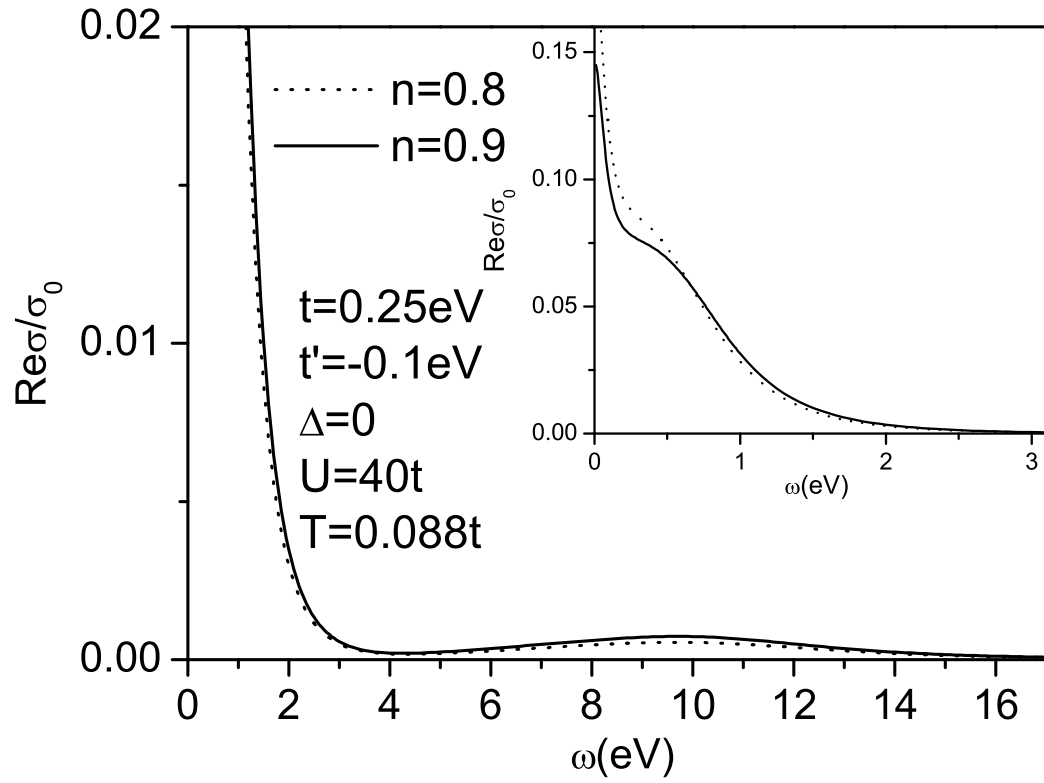


FIG. 8: Real part of optical conductivity for doped Mott insulator ($U = 40t$, $t^0 = 0.4t$, $t = 0.25$ eV) in DMFT approximation. Filling factors are: $n = 0.8$ and $n = 0.9$, temperature $T = 0.088t$. Small frequency behavior is shown in more details at the insert.

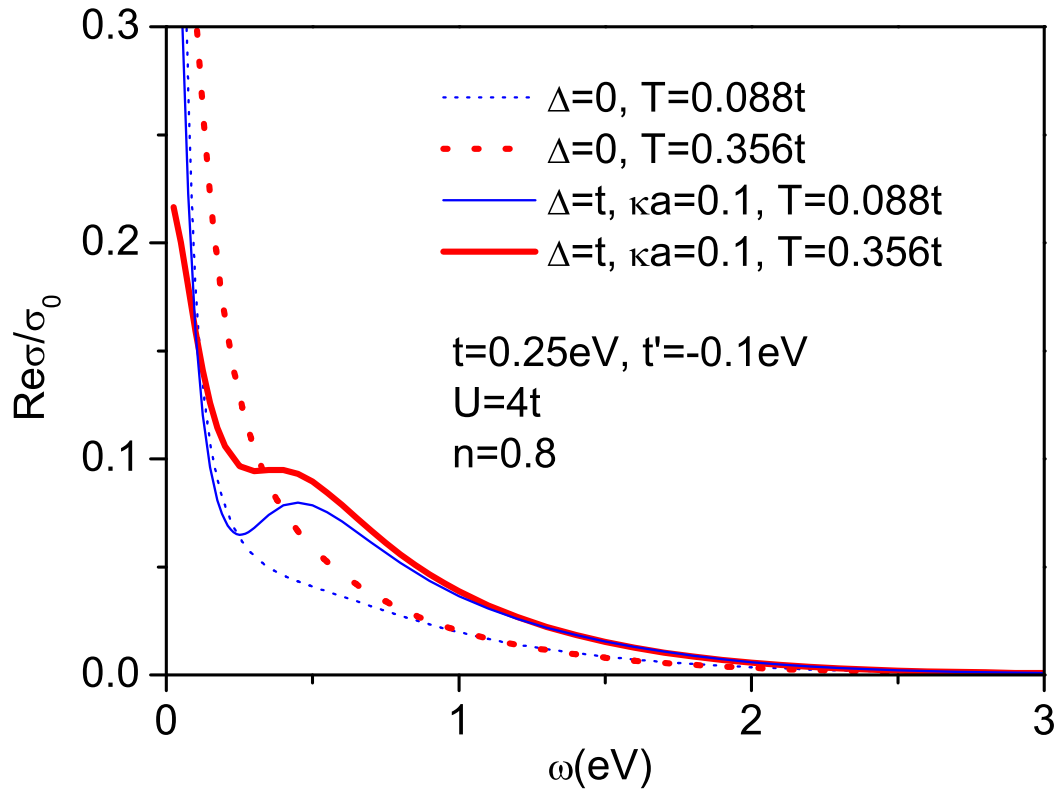


FIG. 9: (Color online) Real part of optical conductivity for correlated metal ($U = 4t, t^0 = 0.4t, t = 0.25 \text{ eV}$) in DMFT+ γ_p approximation for two different temperatures: $T = 0.088t$ and $T = 0.356t$. Pseudogap amplitude $= t$, correlation length $= 10a$, filling factor $n = 0.8$ electrons per atom.

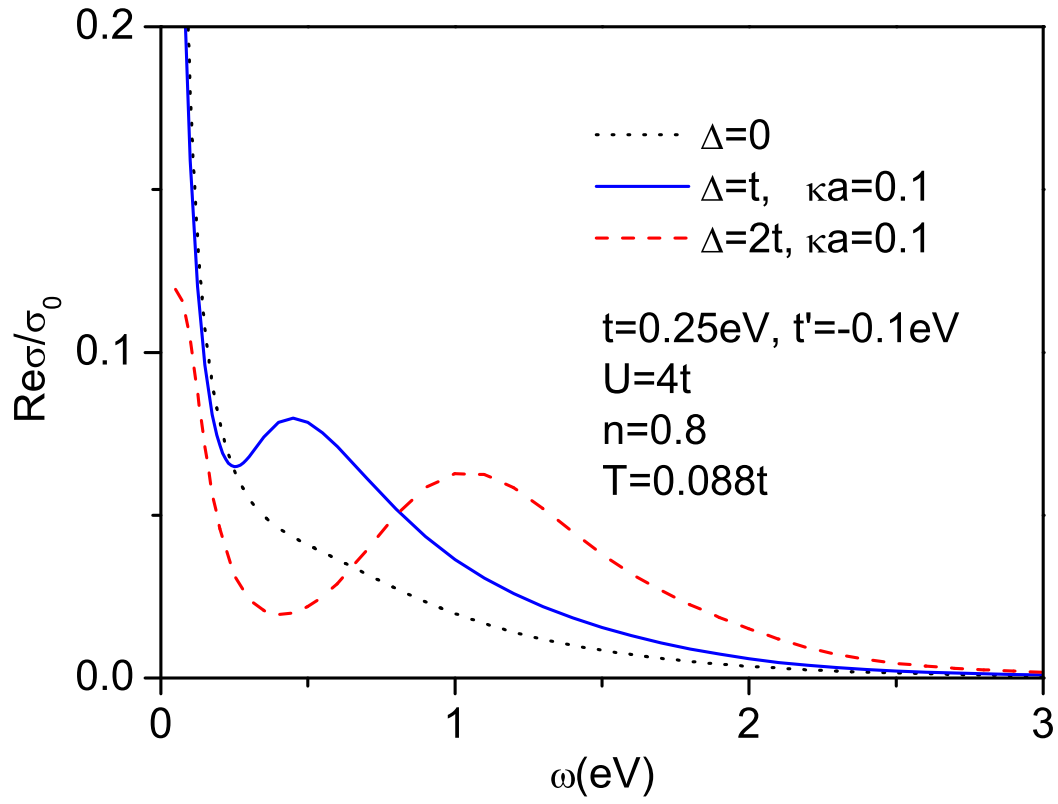


FIG. 10: (Color online) Real part of optical conductivity for correlated metal ($U = 4t, t' = -0.4t, t = 0.25 \text{ eV}$) in DMFT+ γ_p approximation | dependence. Parameters are the same as in Fig. 9, but data are for different values of $\Delta = 0, \Delta = t, \Delta = 2t$, and temperature $T = 0.088t$.

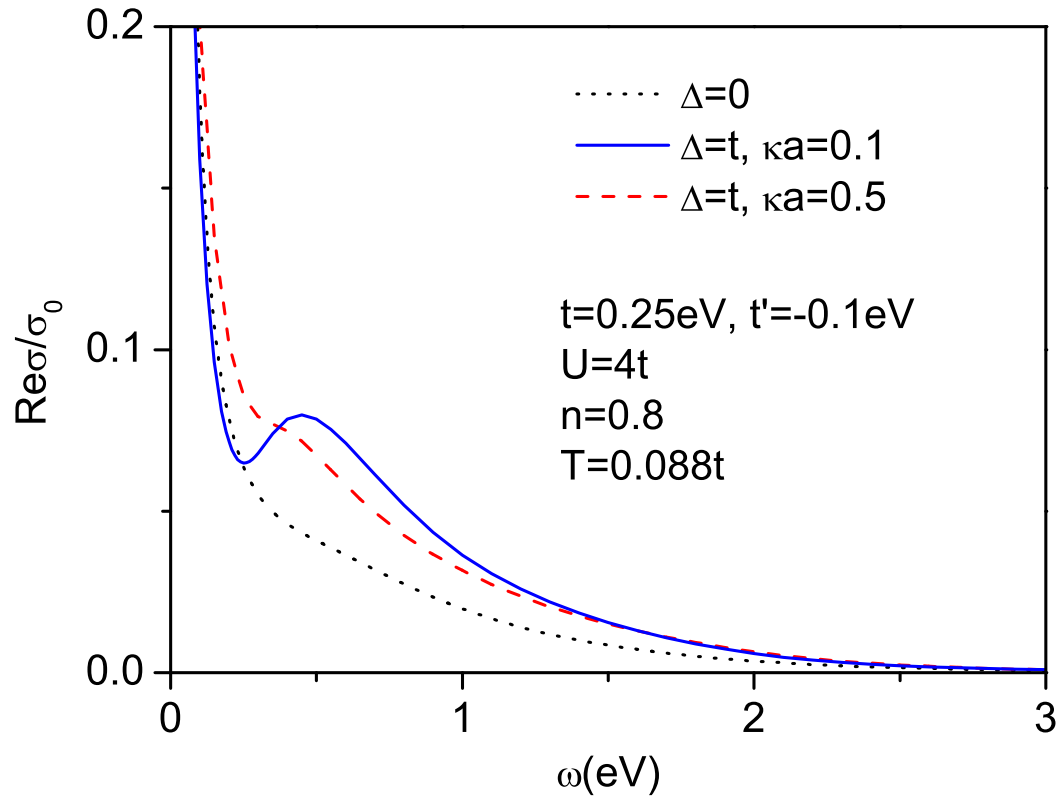


FIG. 11: (Color online) Real part of optical conductivity for correlated metal ($U = 4t$, $t^0 = 0.4t$, $t = 0.25 \text{ eV}$) in DMFT+ p approximation | dependence on correlation length. Parameters are the same as in Fig. 9, but data are for different values of inverse correlation length $\kappa = 1$: $\kappa a = 0.1$ and $\kappa a = 0.5$, and temperature $T = 0.088t$.

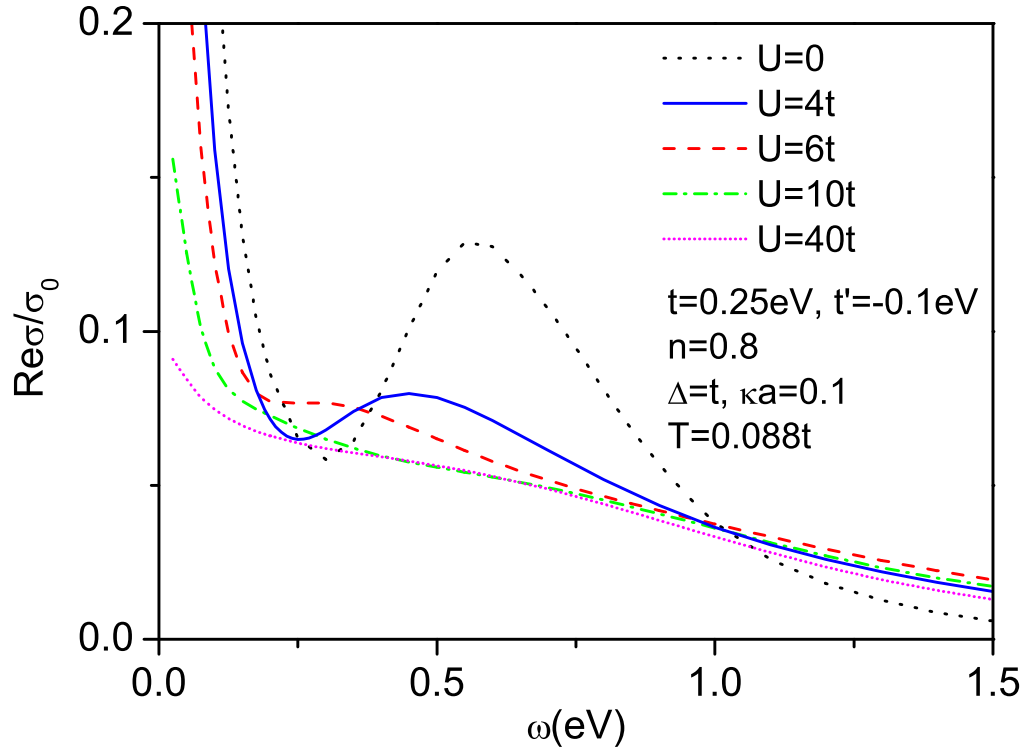


FIG. 12: (Color online) Real part of optical conductivity for correlated metal in DMFT+_p approximation | U dependence. Parameters are the same as in Fig. 9, but data are for different values U : $U=0, U=4t, U=6t, U=10t$ and $U=40t$. Temperature $T=0.088t$.

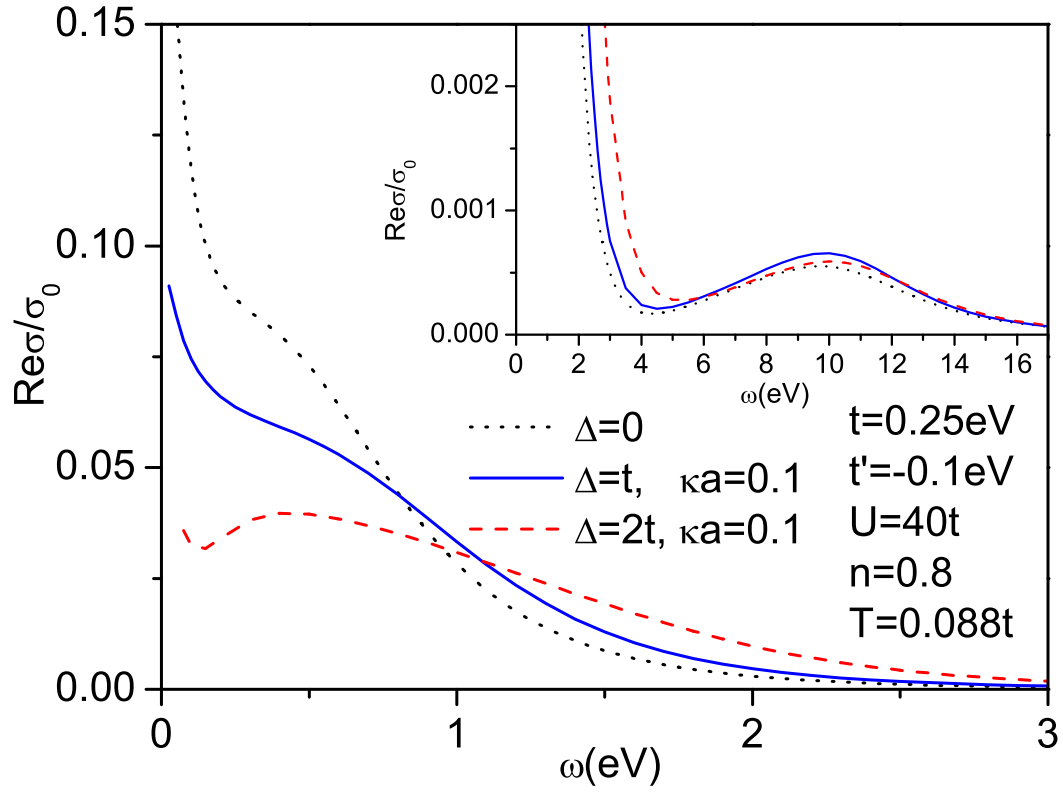


FIG. 13: (Color online) Real part of optical conductivity for doped Mott insulator ($U = 40t$, $t^0 = 0.4t$, $t = 0.25$ eV) in DMFT+ p approximation for different values of $\Delta = 0$, $\Delta = t$, $\Delta = 2t$, and temperature $T = 0.088t$. Correlation length $\xi = 10a$, filling factor $n = 0.8$. Insert: conductivity in a wide frequency interval, including transitions to the upper Hubbard band.

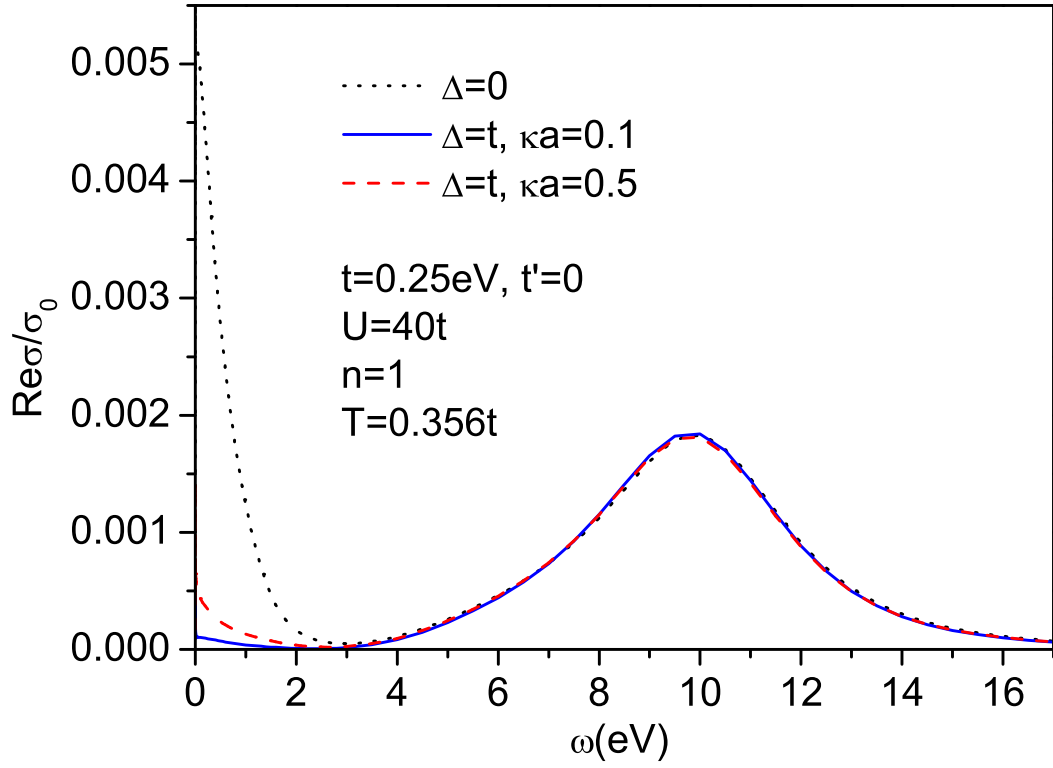


FIG. 14: (Color online) Real part of optical conductivity for doped Mott insulator ($U = 40t$, $t = 0.25 \text{ eV}$; $t' = 0$) in DMFT+ p approximation for different values of inverse correlation length κ^{-1} : $\kappa a = 0.1$ and $\kappa a = 0.5$, temperature $T = 0.356t$ and filling $n = 1$.